Correcting density functional theory for accurate predictions of compound enthalpies of formation: Fitted elemental-phase reference energies

Vladan Stevanović, Stephan Lany, Xiuwen Zhang, and Alex Zunger

Phys. Rev. B **85**, 115104 — Published 7 March 2012

DOI: 10.1103/PhysRevB.85.115104

Correcting Density Functional Theory for Accurate Predictions of Compound Enthalpies of Formation: Fitted elemental-phase Reference Energies (FERE)

Vladan Stevanović and Stephan Lany*
National Renewable Energy Laboratory, Golden, Colorado 80401, USA

Xiuwen Zhang
Department of Physics, Colorado School of Mines, Golden, Colorado 80401, USA

Alex Zunger
University of Colorado, Boulder, Colorado 80309, USA
(Dated: January 19, 2012)

Despite the great success that theoretical approaches based on density functional theory have in describing properties of solid compounds, accurate predictions of the enthalpies of formation (ΔH_f) of insulating and semiconducting solids still remain a challenge. This is mainly due to incomplete error cancellation when computing the total energy differences between the compound total energy and the total energies of its elemental constituents. In this paper we present an approach based on GGA+U calculations, including the spin-orbit coupling, which involves fitted elemental-phase reference energies (FERE) and which significantly improves the error cancellation with compound total energies resulting in accurate values for the compound enthalpies of formation. We use an extensive set of 252 binary compounds with measured ΔH_f values (pnictides, chalcogenides and halides) to obtain FERE energies and show that after the fitting, the 252 enthalpies of formation are reproduced with the mean absolute error MAE=0.054 eV/atom instead of MAE≈0.250 eV/atom resulting from pure GGA calculations. When applied to a set of 55 ternary compounds that were not part of the fitting set the FERE method reproduces their enthalpies of formation with MAE=0.048 eV/atom. Furthermore, we find that contributions to the total energy differences coming from the spin-orbit coupling can be, to a good approximation, separated into purely atomic contributions which do not affect ΔH_f. The FERE method, hence, represents a simple and general approach, as it is computationally equivalent to the cost of pure GGA calculations and applies to virtually all insulating and semiconducting compounds, for predicting compound ΔH_f values with chemical accuracy. We also show that by providing accurate ΔH_f the FERE approach can be applied for accurate predictions of the compound thermodynamic stability or for predictions of Li-ion battery voltages.

PACS numbers:

I. INTRODUCTION

The enthalpy of formation (ΔH_f) of a chemical compound $A_{n_1}B_{n_2}\ldots$ is defined as the change in enthalpy that accompanies the following chemical reaction:

$$n_1\,\mathrm{A} + n_2\,\mathrm{B} + \ldots \longrightarrow \mathrm{A}_{n_1}\mathrm{B}_{n_2}\ldots, \qquad (1)$$

where A, B,... reperesent the pure elements in their conventional reference phases (not free atoms) and n_i stands for the number of atoms of the i-th element in a single formula unit. In many important areas of modern materials science this quantity, i.e. the energy needed to form a compound out of its elemental constituents plays a central role. For example, ΔH_f of a compound, if negative, determines ranges of chemical potentials of its elemental constituents within which the examined compound is thermodynamically stable. This is needed for predicting defect concentrations in a semiconductor material under various realistic growth conditions[1], as well as for predicting the thermodynamic stability of new, not yet synthesized solid-state compounds[2,3]. Furthermore, improving the performance of Li-ion batteries or designing better materials for chemical Hydrogen storage assumes quantitive predictions of the energetics of chemical reactions that involve atomic Li or H_2 molecules[4,5]. In general, to predict accurately the energies needed for chemical reactions to occur (enthalpies of reactions) one ultimately needs to know the ΔH_f values of all chemical compounds involved.

Enthalpies of formation, the subject of this paper, correspond to total energy difference between a compound $A_{n_1}B_{n_2}\ldots$ and the elemental phases A, B,... When all pertain to similar classes of materials, such as all being metallic solids, the calculation of ΔH_f can be performed within one of the standard approximations to density functional theory (DFT), namely the LDA or GGA, which benefit from cancellation of errors associated with similarly imperfect description of bonding in $A_{n_1}B_{n_2}\ldots$ and its constituent solids A, B,... Indeed, GGA works well for ΔH_f of intermetallic compounds[6]. However, when some of elemental constituents of $A_{n_1}B_{n_2}\ldots$ are metals and other nonmetals, as is the case for metal-chalcogenides or metal-pnictides, we may not benefit from systematic cancellation of errors in evaluating the ΔH_f in which case one typically encounters large errors. Unfortunately, simple DFT corrections such as GGA+U

may be problematic as they could apply to the compound but not to the metallic constituents A, B, ... (mixtures of GGA+U for some and GGA for the other have been suggested[7]).

In this paper we present a computationally inexpensive theoretical approach based on GGA+U calculations with fitted elemental-phase reference energies (FERE) which can be used for accurate predictions of the ΔH_f values of binary, ternary and multinary solid compounds involving chemical bonding between metals and nonmetals (such as pnictides, chalcogenides, halides). As we show here, by providing accurate ΔH_f the FERE approach can be applied for accurate predictions of the compound thermodynamic stability with respect to decomposition into the competing phases which can be used for predicting the existence and needed growth conditions for new/unknown compounds[2,3]. Additionally, our method can also be used for accurate predictions of Li-ion battery voltages as we also show in this paper.

II. THE PROBLEM OF PREDICTING THE COMPOUND ENTHALPIES OF FORMATION

Supposed that sufficiently accurate enthalpies are available ΔH_f would simply be determined as the difference of enthalpies of the right- and the left-hand side of Eq. (1). At zero pressure and zero temperature the enthalpy of a system equals its total energy, and the enthalpy of formation is:

$$\Delta H_f(A_{n_1}B_{n_2}\dots) = E_{tot.}(A_{n_1}B_{n_2}\dots) - \sum_i n_i\,\mu_i^0, \quad (2)$$

where $E_{tot.}(A_{n_1}B_{n_2}\dots)$ is the total energy per formula unit of a given compound and μ_i^0 are the total energies per atom of the elements A, B,... in their elemental reference phase. Calculating total energies to chemical accuracy (1 kcal/mol $\approx$ 0.043 eV/atom) is a daunting task and is presently achievable only within computationally very expensive Configuration Interaction (CI) or Quantum Monte Carlo (QMC) approaches and is restricted to systems having a relatively small number of electrons, like light atoms[8]. From Eq. (2), we see, however, that the accurate prediction of ΔH_f does not necessitate extremely accurate total energies, since ΔH_f is not affected by a systematic error cancellation between the elemental reference phases and the compounds, i.e., any *atomic* total-energy error which does not depend on the chemical phase the atom is located in will leave ΔH_f unchanged. Hence, approximate total-energy methods like DFT can be very successful if a systematic error cancellation occurs. For example, Wolverton and Ozoliņš[6] showed that when computing enthalpies of formation of intermetallic alloys, within the two standard approximations to DFT namely the local density approximation (LDA) and the generalized gradient approximation (GGA), the error cancellation is almost exact. In this case one calculates the total energy differences between chemically and physically similar systems, the metallic alloy and its elemental (also metallic) constituents. However, both LDA and GGA fail to reproduce accurately measured ΔH_f values of semiconducting and insulating compounds as shown for the 3d transition metal pnictides and chalcogenides in the upper part of Fig. 1 as well as in Refs.[4,9]. In such cases calculating ΔH_f implies total energy differences between systems that are both chemically and physically very different, the insulating compound versus its constituents such as pure metals and molecular species (e.g. O_2 gas). For example, GGA predicts $\Delta H_f(Al_2O_3) = -3.04$ eV/atom[9], which deviates from the experimental value of -3.48 eV/atom[10] by $+0.44$ eV/atom. Similarly, both LDA and GGA predict ΔH_f of group II and III sulfides too positive by $+0.25$ eV/atom on average[9]. These errors, which exceed considerably the uncertainty of experiments that is generally well below 0.1 eV/atom, can be attributed to the incomplete error cancellation between the total-energies of the compounds $A_{n_1}B_{n_2}\dots$ and the elemental reference phases[9].

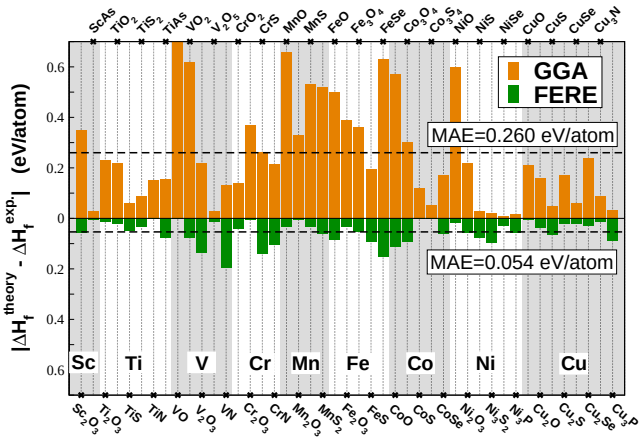

FIG. 1: Histogram showing absolute errors of the GGA (upper part) and of the FERE approach (lower part) in reproducing measured enthalpies of formation[10,11] for 45 binary pnictides and chalcogenides containing 3d transition metals. Dashed lines represent the mean absolute error (MAE) of the two methods corresponding to the full set of 252 binary compounds listed in Tables II and III. Numerical values for the compounds shown in this figure are provided in Table I.

The most striking example of the GGA failure in reproducing experimental ΔH_f are certainly binary pnictides and chalcogenides of 3d transition metals. In the upper part of Fig. 1 absolute deviations of the ΔH_f values calculated in GGA from the experimental ones[10,11] are shown. For 21 out of 45 compounds the GGA errors are in 0.2-0.8 eV/atom range and for VO the error amounts to even $\sim$1 eV/atom. These deviations are unacceptably high as they would lead to serious errors in predictions, both quantitatively and qualitatively. In case of transition metal (TM) compounds, which can oc-

cur in different oxidation states of the TM, there exists an additional source of uncertainty: due to the residual self-interaction error, standard DFT tends to favor energetically the compounds with higher TM oxidation states (lower d-occupancies), which can lead to unrealistic predictions about the stability or instability of compounds with certain compositions[12,13]. Expressing the actual atomic chemical potential by its deviation from the elemental reference state, $\mu_i = \mu_i^0 + \Delta\mu_i$, and using Eq. (2), we obtain the relation $\sum n_i \Delta\mu_i = \Delta \mathrm{H}_f(\mathrm{A}_{n_1}\mathrm{B}_{n_2}\dots)$ for equilibrium conditions, which is shown in Fig. 2 for the case of NiO and Ni_2O_3. We see that in GGA, Ni_2O_3 is more stable than NiO for the entire range of allowed chemical potentials ($\Delta\mu_O \leq 0, \Delta\mu_{Ni} \leq 0$). In other words, GGA predicts, in contrast to the experimental observation, that NiO should spontaneously decompose into Ni_2O_3 by release of Ni or uptake of O from the atomic reservoirs. The instability of the lower oxidations state, e.g., Ni^{+2} (d8) in NiO relative to Ni^{+3} (d7) in Ni_2O_3, can be remedied by the DFT+U method[14], as shown before in Refs.[12,13]. For the direct calculation of $\Delta \mathrm{H}_f$, however, DFT+U suffers from the problem that numerical values for U that correct the relative stability of different oxidation states in the compounds lead to serious errors in the total energies of pure metallic elemental phases which do not cancel when computing $\Delta \mathrm{H}_f$.[30] On the other hand, applying computationally much more expensive hybrid functionals[15] is shown to improve only slightly the $\Delta \mathrm{H}_f$ values and the remaining error is still relatively large[4].

Another alternative approach for computing $\Delta \mathrm{H}_f$ has been recently proposed[7]. It mixes GGA and GGA+U exchange-correlation functionals by dividing compounds and elemental substances into groups within which the accurate description is provided by either GGA or GGA+U. Enthalpies of formation are than computed by combining the total energies obtained by GGA and GGA+U (renormalized in a special way to be compatible with each other). In this approach the Hubbard U values are element dependent and are fitted to a set of experimental enthalpies of reactions. It has been shown that the measured enthalpies of formation of 49 ternary oxides can be reproduced with the average error of 0.045 eV/atom.

Also recently, Lany[9] showed that accurate $\Delta \mathrm{H}_f$ values of insulating and semiconducting compounds can be obtained by fitting a set of elemental-reference energies (μ^0) that systematically improve the error cancelation in Eq. (2). In the present work we build on, and extend the work of Lany[9] from 14 to 50 elements, including 21 transition metals, fitted to a set of 252 measured $\Delta \mathrm{H}_f$ for binary compounds , and, in addition, we address three important issues: (*i*) how to determine the value of the Hubbard U needed for computing total energies of transition metal compounds that will lead to accurate enthalpies of formation, (*ii*) to what extent the method that we propose can be predictive, or in other words, what is its accuracy when applied to compounds not used for fitting; and (*iii*) what is the effect of spin-orbit interactions on calculated compound enthalpies of formation.

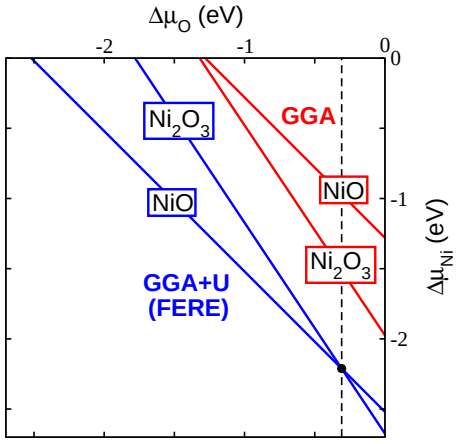

FIG. 2: The relation of the chemical potentials $\Delta\mu$ of Ni and O for equilibrium with the NiO and Ni_2O_3 compound phases, as calculated in GGA and in the present FERE method based on GGA+U compound energies. In GGA, NiO is unstable against Ni_2O_3 for the full range of allowed chemical potentials $\Delta\mu \leq 0$. The correct phase stability of NiO is recovered in the present method.

Following Ref.[9] the FERE energies are obtained by solving the linear least-squares problem

$$\Delta \mathrm{H}_f^{exp.}(\mathrm{A}_{n_1}\mathrm{B}_{n_2}\dots) = \mathrm{E}_{tot.}^{GGA+U}(\mathrm{A}_{n_1}\mathrm{B}_{n_2}\dots) - \sum_i n_i\,\mu_i^{FERE}, \quad (3)$$

for the elemental-phase energies μ_i^{FERE} that optimally cancel total-energy errors with the compound energies $\mathrm{E}_{tot.}^{GGA+U}$ which are computed using the experimental crystal structures with the GGA+U optimized lattice vectors and atomic positions. Our choice for the value of the Hubbard U parameter (U = 3 eV for all transition metals except Cu and Ag for which U = 5 eV) is discussed in details in Sec. V A. The experimental values $\Delta \mathrm{H}_f^{exp.}$ are taken from Refs.[10,11].

The FERE energies can be expressed as an energy-shifts $\delta\mu_i^{FERE}$ relative to the calculated elemental total-energies

$$\mu_i^{FERE} = \mu_i^{GGA+U} + \delta\mu_i^{FERE}, \quad (4)$$

which can be used to express the FERE predicted heat of formation as a correction of the directly calculated $\Delta \mathrm{H}_f^{GGA+U}$ by a sum of the energy shifts $\delta\mu_i^{FERE}$ weighted by the stoichiometric factors n_i of the respective elements in the compound:

$$\Delta \mathrm{H}_f^{FERE}(\mathrm{A}_{n_1}\mathrm{B}_{n_2}\dots) = \Delta \mathrm{H}_f^{GGA+U}(\mathrm{A}_{n_1}\mathrm{B}_{n_2}\dots) - \sum_i n_i\,\delta\mu_i^{FERE}. \quad (5)$$

TABLE I: Comparison of measured ΔH_f[10,11] and those resulting from pure GGA and the FERE method (see Eq. (5)) on a set of 45 binary pnictides and chalcogenides containing 3d transition metals. All numbers are given in eV/atom. Conversion factor to [kJ/mol] is ≈96.5*N, where N stands for the number of atoms per compound formula unit. Absolute errors of the two approaches are presented graphically in Fig. 1.

Compound	ΔH_f^{GGA}	ΔH_f^{FERE}	ΔH_f^{exp}	Compound	ΔH_f^{GGA}	ΔH_f^{FERE}	ΔH_f^{exp}
Sc_2O_3	-3.59	-3.88	-3.94	Fe_3O_4	-1.30	-1.71	-1.66
ScAs	-1.42	-1.39	-1.39	FeS	-0.32	-0.61	-0.52
Ti_2O_3	-2.92	-3.14	-3.15	FeSe	+0.24	-0.24	-0.39
TiO_2	-3.04	-3.24	-3.26	CoO	-0.66	-1.34	-1.23
TiS	-1.47	-1.46	-1.41	Co_3O_4	-1.02	-1.41	-1.32
TiS_2	-1.32	-1.44	-1.41	CoS	-0.31	-0.43	-0.43
TiN	-1.74	-1.58	-1.58	Co_3S_4	-0.48	-0.53	-0.53
TiAs	-0.93	-0.70	-0.78	CoSe	-0.15	-0.26	-0.32
VO	-1.06	-2.26	-2.24	NiO	-0.64	-1.26	-1.24
VO_2	-1.85	-2.55	-2.47	Ni_2O_3	-0.79	-1.07	-1.01
V_2O_3	-2.30	-2.66	-2.52	NiS	-0.39	-0.50	-0.42
V_2O_5	-2.27	-2.28	-2.30	Ni_3S_2	-0.40	-0.52	-0.42
VN	-0.99	-0.93	-1.12	NiSe	-0.30	-0.34	-0.31
CrO_2	-1.92	-2.03	-2.06	Ni_3P	-0.56	-0.48	-0.54
Cr_2O_3	-1.99	-2.36	-2.36	CuO	-0.61	-0.81	-0.82
CrS	-0.54	-0.95	-0.81	Cu_2O	-0.42	-0.62	-0.58
CrN	-0.43	-0.54	-0.65	CuS	-0.23	-0.34	-0.28
MnO	-1.34	-2.03	-2.00	Cu_2S	-0.11	-0.30	-0.28
Mn_2O_3	-1.66	-2.00	-1.99	CuSe	-0.14	-0.19	-0.21
MnS	-0.58	-1.14	-1.11	Cu_2Se	+0.04	-0.18	-0.21
MnS_2	-0.47	-0.78	-0.72	Cu_3N	+0.28	+0.18	+0.19
FeO	-0.91	-1.32	-1.41	Cu_3P	-0.14	-0.08	-0.17
Fe_2O_3	-1.32	-1.74	-1.71				

The $\delta\mu_i^{FERE}$ values that are obtained in this work are given in Fig. 3. We emphasize, however, that the energy shifts $\delta\mu_i^{FERE}$ are not meant to improve the absolute total-energies for the elemental phases, but rather are constructed such to optimize the systematic error cancellation with the total-energies of the compounds. Moreover, the GGA+U total energies of the pure elemental phases are used in this work only as a reference point for the use of the corrections $\delta\mu_i^{FERE}$, and that in general one cannot expect that U=3 is reasonable choice for pure metals.

We solve the least-square problem of Eq. (3) for 50 elements in their conventional reference phase using a set of 252 *binary* compounds. We cover the majority of the standard, earth abundant elements including the full list of, for DFT "problematic", 3d transitions metals. This list shown in Fig. 3 also includes a good portion of the 4d and 5d transition metals. We show that the FERE energies obtained in this way significantly improve the ΔH_f of the binary compounds leading to the mean absolute error (MAE) of 0.054 eV/atom (root-mean-square error, rms=0.070 eV/atom). Furthermore, we demonstrate the predictive power of our approach by computing the ΔH_f values for 55 *ternary* compounds with measured enthalpies of formation and show that the FERE approach reproduces accurately the experimental values with MAE=0.048 eV/atom (rms=0.059 eV/atom) as shown in Fig. 4. Furthermore, since our set contains a number of elements for which the contribution of spin-orbit coupling cannot be neglected we also performed the analysis of the magnitude of this contribution to ΔH_f values and found that to a good approximation spin-orbit coupling energy in a compound can be separated in purely atomic contributions which, as already said, to a good approximation cancel when calculating the total energy differences in Eq. (2).

The FERE method corrects for the difficulty of DFT to determine accurate energy differences when an atom is located in different bonding environments. We are interested metal-nonmetal compounds (with well-defined cations and anions). The FERE method then determines fictitious energies for the elemental phases (metallic, molecular, and covalent bonding), such that they are described consistently with the DFT energy of the same atom in an ionic bonding environment. Our FERE energies do not apply, e.g., for ΔH_f of metallic alloys, where all total-energies are determined for systems with metallic bonding. Here, direct calculation in GGA is known to

be accurate[6]. Notably, the variation of the ionic vs covalent character within a series of ionic compounds (e.g., MgO vs ZnO, ZnO vs ZnSe) does not noticeably affect the ability to fit all elements with one single μ^{FERE}, as long as one can clearly assign a formal oxidation number to the element in the compound (e.g., Mg^{2+}, Zn^{2+}, O^{2-}, Se^{2-}). This indicates that DFT consistently describes (i.e., the DFT total-energy error is constant for) "ionic" compounds with a varying degree of covalency in the bonding. However, this systematic error cancellation breaks down towards the limit of perfect covalency, as seen, e.g., by the large difference of 0.43 eV between μ^{FERE} for Si^{4+} and the directly calculated energy of elemental Si having a formal oxidation number of 0. Thus, one can in general expect FERE only to work for a fixed oxidation number of the element. Note that in case of transition metals it is only thanks to GGA+U that a certain range of oxidation states are covered, e.g. Ni^{2+}/Ni^{3+}, or V^{2+} trough V^{5+}, as long as we stay within the realm of compounds with metal-nonmetal bonding.

III. COMPUTATIONAL APPROACH

The standard scheme, frequently used in DFT calculations has been employed also in this work. The PBE exchange-correlation functional[16] is used, both in GGA and GGA+U calculations[14]. All calculations are performed within the projected augmented wave (PAW) method[17] as implemented in VASP computer code[18]. Constant U=3 eV value is used for all transition metals except Cu and Ag for which we use U=5 eV value (for justification see the discussion in Section V A). For all non-transition elements as well as for Zn, Cd and Hg, the Hubbard U parameter is set to zero. A Monkhorst-Pack **k**-point sampling[19] is applied with all total energies converged within 3 meV/atom with respect to the number of **k**-points. The plane wave cutoff is set to the value 30 % higher than the highest suggested by the employed pseudopotentials (e.g. 520 eV for oxygen). Spin degrees of freedom are treated explicitly, and the limited search for the ground state magnetic configurations has been performed. Experimentally determined magnetic configurations are used whenever possible (mostly for binary compounds) and in the cases where there is no experimental data (e.g. ternaries) the search is done on a primitive unit cell by initializing magnetic moments in different ways including both high and low spin values as well as up to 10 different relative orientations (ferro, anti-ferro and different random realizations) and letting the system relax. We find that the energy differences associated with different magnetic configurations are typically of the order of ∼0.01-0.02 eV/atom and do not contribute appreciably to relatively large errors that ab-initio methods usually make. Full list of all chemical elements included in this work as well as the list of corresponding pseudopotentials used in calculations is presented in Table VI of the Appendix. As already noted total energies of all compounds considered in this work are computed on their experimental structures with GGA+U optimized lattice constants and atomic positions. The structures are taken from the Inorganic Crystal Structure Database (ICSD)[20,21]. For GeO_2 we consider both the hexagonal and the tetragonal phase, total energy of Al_2SiO_5 we compute for all three Andalusite, Kyanite and Silimanite phases, and $CaSiO_3$ we consider both in wollastonite and pseudo-wollastonite structures.

IV. RESULTS OF THE FITTING

As we show in this work, the errors in computing compound ΔH_f can be corrected for, by introducing semiempirical FERE energies and obtaining their values by solving the least-square fitting problem of Eq. (3). A full list of 252 binary compounds, comprising 50 different elements, that we used for fitting, is presented in Table II and Table III. We consider only "ionic" compounds with elements from groups I-IV of the periodic table as cations and the elements from groups V, VI and VII as anions. The system of 252 linear equations with 50 unknown μ_i^{FERE} values we solve using the standard least-square routine. The resulting set of 50 fitted $\{\mu_i^{FERE}\}$ values is shown in Fig. 3 in terms of corrections $\delta\mu_i^{FERE}$ defined in Eq. (4). The absolute μ_i^{FERE} values are given in Table VI in the Appendix. However, the absolute values should be used with caution as they correspond to a particular numerical scheme (discussed already) and to a particular choice of pseudopotentials that are also listed in Table VI in the Appendix. On the other hand, the corrections $\{\delta\mu_i^{FERE}\}$ to the GGA+U total energies of pure elements in their conventional reference phases are more general and should be the same for equivalent implementations of the GGA+U method (e.g. within the PAW formalism). As shown in Fig. 3 the magnitudes of $\delta\mu_i^{FERE}$ are typically in the 0-0.6 eV range as already found by Lany[9] for a set of 14 main group elements. However, there are cases such as Au, Zr, Hf, where the corrections are larger and amount to ∼0.7-1.2 eV. Using the values tabulated in Fig. 3 the experimental enthalpies of formation of the compounds that belong to the fitting set are reproduced with MAE= 0.054 eV/atom (rms=0.070 eV/atom). When translated to [kJ/mol], which are the standard units used in chemistry, MAE∼ 5.21∗N kJ/mol, where N stands for the number of atoms in one formula unit. Therefore, the expected error of the FERE method for a binary compound having, for example 3 atoms per formula unit amounts to ∼15 kJ/mol. Table II and Table III list the FERE enthalpies of formation for our set of binary compounds together with the experimental values. There is a relatively small fraction of binary compounds belonging to the fitting set, 20 out of 252 (shown in bold), for which the remaining FERE error exceeds two times the MAE value. These errors are not very large and are all in 0.1-0.2 eV/atom range. For some of these larger errors there is a relatively simple physical explanation.

TABLE II: Comparison of ΔH_f values (in eV/atom) from experiment and calculated using the FERE method for 252 binary compounds used for fitting. Experimental data are from compilations of Refs.[10,11]. Compounds for which the deviation of ΔH_f^{FERE} from experiment is more than double the MAE=0.054 eV/atom are shown in bold letters (20 compounds). For GeO_2 we consider both hexagonal (h) and tetragonal (t) phase. Conversion factor to kJ/mol is $\sim 96.5*N$, where N stands for the number of atoms per compound formula unit.

Compound	ΔH_f^{FERE}	ΔH_f^{exp}	Compound	ΔH_f^{FERE}	ΔH_f^{exp}	Compound	ΔH_f^{FERE}	ΔH_f^{exp}	Compound	ΔH_f^{FERE}	ΔH_f^{exp}
Ag_2O	-0.15	-0.11	Co_3S_4	-0.53	-0.53	HgS	-0.28	-0.30	$MgCl_2$	-2.19	-2.21
Ag_2O_2	-0.10	-0.06	CrF_4	-2.56	-2.58	HgSe	-0.27	-0.24	MgF_2	-3.86	-3.88
Ag_2S	-0.12	-0.11	**CrN**	-0.54	-0.65	HgTe	-0.20	-0.22	MgO	-3.15	-3.11
Ag_2Se	-0.08	-0.15	CrO_2	-2.03	-2.07	InAs	-0.25	-0.31	MgS	-1.78	-1.79
AlAs	-0.65	-0.61	CrS	-0.95	-0.81	InN	-0.03	-0.10	MgSe	-1.49	-1.52
$AlCl_3$	-1.85	-1.82	Cr_2O_3	-2.37	-2.36	InP	-0.31	-0.39	MgTe	-1.10	-1.08
AlF_3	-3.86	-3.90	CuF_2	-1.86	-1.88	InS	-0.78	-0.70	**Mg_3As_2**	-0.80	-0.91
AlN	-1.68	-1.61	CuO	-0.81	-0.82	InSb	-0.24	-0.16	Mg_3Bi_2	-0.40	-0.32
AlP	-0.86	-0.85	CuS	-0.34	-0.28	InSe	-0.70	-0.62	Mg_3N_2	-1.06	-0.96
Al_2O_3	-3.46	-3.47	CuSe	-0.19	-0.21	InTe	-0.44	-0.50	Mg_3P_2	-0.92	-0.96
Al_2S_3	-1.42	-1.50	Cu_2O	-0.62	-0.58	In_2O_3	-1.92	-1.92	**Mg_3Sb_2**	-0.64	-0.49
Al_2Se_3	-1.09	-1.18	Cu_2S	-0.30	-0.28	In_2S_3	-0.80	-0.74	MnO	-2.03	-2.00
Al_2Te_3	-0.66	-0.68	Cu_2Sb	-0.00	-0.04	In_2Se_3	-0.64	-0.67	MnS	-1.14	-1.11
AuCl	-0.14	-0.18	Cu_2Se	-0.18	-0.21	In_2Te_3	-0.33	-0.41	MnS_2	-0.78	-0.72
$AuCl_3$	-0.29	-0.30	Cu_2Te	-0.06	0.07	IrO_2	-0.99	-0.95	**MnSb**	-0.15	-0.26
AuF_3	-1.02	-0.94	Cu_3N	0.18	0.19	IrS_2	-0.52	-0.48	Mn_2O_3	-2.00	-1.99
BaO	-2.85	-2.86	Cu_3P	-0.08	-0.17	Ir_2S_3	-0.43	-0.49	NaCl	-2.04	-2.13
BaO_2	-2.15	-2.19	Cu_3Sb	0.03	-0.02	KCl	-2.22	-2.26	NaF	-2.94	-2.97
BaS	-2.41	-2.38	FeF_2	-2.56	-2.46	KF	-2.96	-2.94	NaSb	-0.37	-0.33
BeO	-3.05	-3.14	FeO	-1.32	-1.41	KSb	-0.50	-0.43	$NaTe_3$	-0.37	-0.35
BeS	-1.30	-1.21	FeS	-0.61	-0.52	**KSb_2**	-0.25	-0.37	Na_2O	-1.44	-1.43
Be_3N_2	-1.22	-1.22	**FeSe**	-0.24	-0.39	K_2O	-1.29	-1.25	Na_2O_2	-1.29	-1.32
$CaCl_2$	-2.67	-2.75	Fe_2O_3	-1.74	-1.71	K_2O_2	-1.30	-1.28	Na_2S	-1.28	-1.26
CaF_2	-4.19	-4.21	Fe_3O_4	-1.71	-1.66	K_2S	-1.30	-1.31	Na_2S_2	-1.02	-1.03
CaO	-3.28	-3.29	**GaAs**	-0.48	-0.37	K_2S_2	-1.15	-1.12	Na_2Se	-1.22	-1.18
CaS	-2.41	-2.45	$GaCl_3$	-1.43	-1.36	K_2Se	-1.28	-1.36	Na_2Se_2	-0.92	-0.97
Ca_3N_2	-0.95	-0.91	**GaF_3**	-2.90	-3.01	K_3As	-0.45	-0.48	Na_3As	-0.50	-0.53
Ca_3P_2	-1.26	-1.22	GaN	-0.72	-0.81	K_3Bi	-0.52	-0.60	Na_3Bi	-0.48	-0.46
$CdCl_2$	-1.35	-1.35	GaP	-0.63	-0.53	K_3Sb	-0.56	-0.47	Na_3Sb	-0.58	-0.53
CdF_2	-2.43	-2.42	GaS	-1.05	-1.09	K_5Sb_4	-0.53	-0.44	NbN	-1.17	-1.22
CdO	-1.33	-1.34	**GaSb**	-0.40	-0.22	$LaCl_3$	-2.74	-2.78	NbO_2	-2.79	-2.75
CdS	-0.88	-0.78	GaSe	-0.89	-0.83	**LaN**	-1.43	-1.57	Nb_2O_5	-2.84	-2.81
CdSb	-0.13	-0.07	Ga_2O_3	-2.26	-2.26	LaS	-2.42	-2.36	NiF_2	-2.25	-2.25
CdSe	-0.77	-0.75	Ga_2S_3	-1.00	-1.07	La_2O_3	-3.77	-3.72	NiO	-1.26	-1.24
CdTe	-0.57	-0.48	Ga_2Se_3	-0.80	-0.85	La_2S_3	-2.48	-2.51	NiS	-0.51	-0.43
Cd_3As_2	-0.15	-0.08	GeO_2(h)	-1.86	-1.90	**La_2Te_3**	-1.74	-1.63	NiSb	-0.27	-0.34
Cd_3N_2	0.41	0.33	GeO_2(t)	-1.92	-2.00	LiCl	-2.05	-2.12	NiSe	-0.34	-0.31
Cd_3P_2	-0.17	-0.24	**GeS**	-0.54	-0.39	LiF	-3.17	-3.19	NiTe	-0.22	-0.28
CoF_2	-2.29	-2.39	GeS_2	-0.58	-0.66	Li_2O	-2.07	-2.07	Ni_2O_3	-1.07	-1.01
CoF_3	-2.15	-2.10	GeSe	-0.42	-0.48	Li_2O_2	-1.63	-1.64	Ni_2Te_3	-0.21	-0.30
CoO	-1.34	-1.23	Ge_3N_4	-0.14	-0.09	Li_2S	-1.55	-1.52	Ni_3P	-0.48	-0.54
CoS	-0.43	-0.43	HfN	-1.90	-1.91	Li_2Se	-1.41	-1.45	Ni_3S_2	-0.52	-0.42
$CoSb_3$	0.01	-0.17	HfO_2	-3.96	-3.95	Li_3Bi	-0.64	-0.60	$PdCl_2$	-0.65	-0.69
CoSe	-0.26	-0.32	$HgCl_2$	-0.80	-0.77	Li_3N	-0.51	-0.43	**PdO**	-0.58	-0.44
Co_3O_4	-1.41	-1.32	HgO	-0.47	-0.47	Li_3Sb	-0.78	-0.83	PdS	-0.37	-0.39

TABLE III: Table II continued.

Compound	ΔH_f^{FERE}	ΔH_f^{exp}	Compound	ΔH_f^{FERE}	ΔH_f^{exp}	Compound	ΔH_f^{FERE}	ΔH_f^{exp}	Compound	ΔH_f^{FERE}	ΔH_f^{exp}
PdS_2	-0.32	-0.28	Rh_2S_3	-0.48	-0.54	Sr_2Bi	-1.00	-1.08	YCl_3	-2.65	-2.59
Pd_4S	-0.07	-0.14	ScAs	-1.39	-1.39	Sr_2Sb	-1.15	-1.11	YF_3	-4.45	-4.45
PtO	-0.37	-0.37	$ScCl_3$	-2.44	-2.40	TaN	-1.25	-1.30	Y_2O_3	-3.92	-3.95
PtO_2	-0.57	-0.57	ScF_3	-4.26	-4.22	TaS_2	-1.29	-1.22	$ZnCl_2$	-1.43	-1.43
PtS	-0.41	-0.42	Sc_2O_3	-3.88	-3.94	TiAs	-0.70	-0.78	ZnF_2	-2.57	-2.64
PtS_2	-0.34	-0.38	SiO_2	-3.06	-3.13	$TiCl_4$	-1.78	-1.70	ZnO	-1.78	-1.81
Pt_3O_4	-0.45	-0.40	SiS_2	-0.91	-0.88	TiN	-1.58	-1.58	ZnP_2	-0.23	-0.21
RbCl	-2.20	-2.26	$SiSe_2$	-0.55	-0.61	TiO_2	-3.24	-3.26	ZnS	-1.09	-1.07
RbF	-2.90	-2.89	Si_3N_4	-1.18	-1.10	TiS	-1.46	-1.41	ZnSb	-0.15	-0.08
RbSb	-0.49	-0.52	SnO	-1.51	-1.48	TiS_2	-1.44	-1.41	ZnSe	-0.89	-0.85
$RbSb_2$	-0.25	-0.35	$\mathbf{SnO_2}$	-1.86	-1.97	Ti_2O_3	-3.14	-3.15	ZnTe	-0.62	-0.61
Rb_2O	-1.17	-1.17	SnS	-0.61	-0.57	$\mathbf{VF_4}$	-3.03	-2.91	Zn_3As_2	-0.21	-0.28
Rb_2O_2	-1.24	-1.22	SnS_2	-0.53	-0.53	**VN**	-0.93	-1.13	Zn_3N_2	-0.07	-0.05
Rb_2S	-1.24	-1.25	SnSe	-0.52	-0.47	VO	-2.24	-2.24	Zn_3P_2	-0.35	-0.33
Rb_3Sb	-0.54	-0.45	$SnSe_2$	-0.37	-0.43	VO_2	-2.55	-2.47	ZrN	-1.91	-1.89
$RhCl_3$	-0.83	-0.78	SrO	-3.11	-3.07	$\mathbf{V_2O_3}$	-2.67	-2.53	ZrO_2	-3.81	-3.80
RhO_2	-0.84	-0.85	SrO_2	-2.19	-2.19	V_2O_5	-2.28	-2.29	ZrS_2	-1.93	-1.96
Rh_2O_3	-0.87	-0.84	SrS	-2.47	-2.45	YAs	-1.67	-1.68	Mn_3O_4	-2.08	-2.05

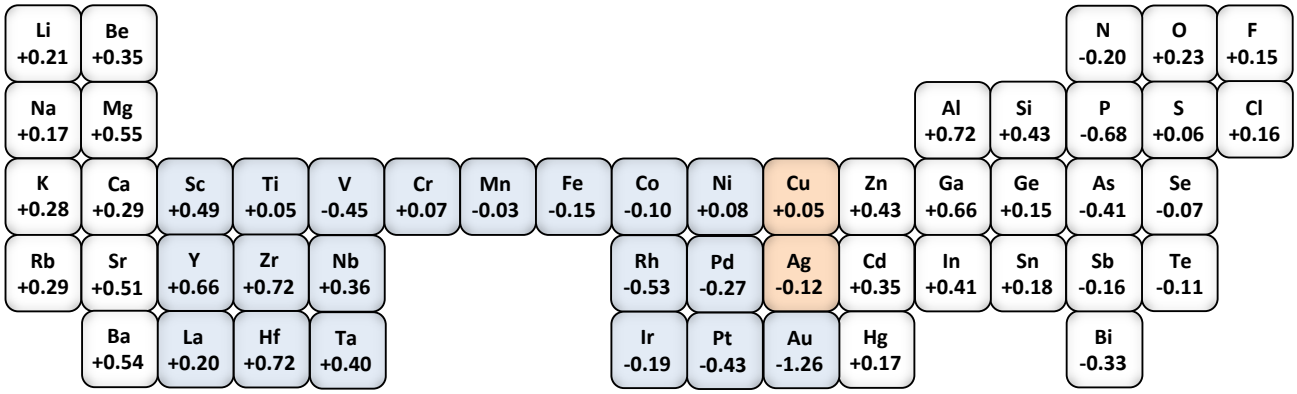

FIG. 3: Part of the periodic table listing the $\delta\mu_i^{FERE}$ values (in eV) of Eq. (4) for 50 chemical elements. Colors denote the values of the Hubbard U parameter used in the calculations: U=3 eV – light blue, U=5 eV – orange, and U=0 eV – light grey. Absolute $\{\mu_i^{FERE}\}$ values are given in Table VI of the Appendix.

In 7 out these 20 compounds the anion is either Sb or As. Both elements appear in the fitting set in different oxidation states and the errors are due to U=0 eV value as already discussed. Similarly, Sn, for which also U=0 eV, appears in 2+ and 4+ oxidation states and a somewhat larger 0.110 eV/atom error appears for SnO_2. For the other 12 cases we suggest possible experimental reconsideration of their ΔH_f. Again, these errors are not exceedingly large compared to those of pure GGA or GGA+U, but it is certainly possible that one inaccurate experimental value drives the fit and affects the rest of the results (e.g. in the case of Vanadium). However, as already mentioned, most of these errors fall in the ∼0.1 eV/atom range leading to a rather good overall performance of the FERE method. Comparison of the performance of the FERE method with GGA on a subset of binary pnictides and chalcogenides containing 3d transition metals is shown graphically in Fig. 1 and numerically in Table I.

The work from Ref.[7] relies on the previous work of Wang *et al.*[13] and assumes the following: (*i*) it uses the value of the oxygen energy (in our language μ_O^0) that has been fitted by Wang *et al.* to reproduce measured enthalpies of formation of 6 main-group metal oxides (CaO, Li_2O, MgO, Al_2O_3, SiO_2 and Na_2O) using pure GGA total energies for metals, (*ii*) the fitted μ_O^0 is then employed

in fitting the element dependent Hubbard U parameters for transition metals to reproduce measured enthalpies of chemical reactions in which given transition metal M changes its oxidation state $MO_x + \frac{y-x}{2}O_2 \rightarrow MO_y$. In order to calculate ΔH_f, the GGA+U energy is taken for compounds with localized orbitals, but the GGA energy for delocalized orbitals in the metallic phase. In order to make the latter compatible with the GGA+U energy, a correction based on experimental data is applied to the GGA energy. In essence, the main difference between both methods is that in Jain et al. fit only the energies of the O_2 molecule and of the transition metals, whereas we fit all elemental energies, including main group metals. A secondary difference is that the approach of Jain et al., as implemented in practice, uses an element-dependent U, whereas we find as a result of our calculations that a uniform U value (except for Ag and Cu) is sufficient in the FERE approach to correct DFT errors relative to experimental formation enthalpies of ∼250 binary compounds. While the two approaches are obviously closely related, we think that our approach is both simpler and more consistent.

V. DISCUSSION

A. The value of the Hubbard U

Values for the Hubbard U parameter that we use require a more detailed discussion. Initially, we allowed the Hubbard U parameters to depend on the chemical identity of transition metals and we treated them as fitting parameters to yield the correct crossing points between different stoichiometries of TM oxides, i.e. the O chemical potential at which the stable phase changes (see Fig. 2). Except for Cu and Ag, we obtained values for U between 2.5 and 3.5 eV for all TM. Since the variation of U of ±0.5 eV resulting from the fit lies within the range that could result from the uncertainty of the experimental data, we used a constant value of U=3.0 eV for all TM, except for Cu and Ag, for which we use U=5 eV. For the compounds of the group IIb elements Zn, Cd, and Hg, as well as for all main group elements, we use GGA without DFT+U.

Fixing the U values is beneficial as it allows to develop a scheme that can be applied to different families of semiconducting and insulating compounds, not only to oxides or other chalcogenides separately, but to oxides, other chalcogenides, pnictides and halides at the same time. Of course, the fixed U values (3 and 5 eV), in conjuction with fitted $\{\delta\mu^{FERE}\}$, are good for thermochemistry, and are not meant for band-gap predictions.

The fact that this "thermochemical" U to a good approximation "does not recognize" differences in the types of chemical compounds and in chemical identities of elements deserves a closer look into the foundations of GGA and GGA+U which is beyond the scope of this paper. However, it would be very interesting to analyze our findings in terms of results of more accurate theoretical approaches such as Quantum Monte Carlo for example.

B. Finite temperature effects

Equations (3)-(5) are formulated in the T→0 limit. However, for the experimental enthalpies of formation (see Eq. (3)) we use values, compiled in Refs.[10,11], that correspond to *standard* conditions, meaning T=298 K and $p = 1$ atm. Therefore, $\Delta H_f^{exp.}$ contain contributions coming, in the case of ordered compounds, from enthalpy of the vibrational motion. Reason for taking standard $\Delta H_f^{exp.}$ lays in the availability of the data compared to much more scarce $\Delta H_f^{exp.}$ values reported (extrapolated) at T=0 K. As noted by Lany[9] the error that is introduced is typically smaller than 0.03 eV/atom which is less than the MAE of our FERE approach and therefore, its contribution is of no significance in the context of this work. On the other hand, the enthalpy of the zero-point motion, which could contribute significantly (∼0.1 eV/atom) to the incomplete error cancellation in Eq. (2) if the first row diatomic molecules are involved, is automatically taken care of by our fitting procedure (Eq. (3)) and is included in the fitted μ_i^{FERE} values.

Another important finite temperature effect that could be of importance for ternary and multinary crystalline compounds is the possibility of atomic disorder. For example, in A_2BX_4 (X=O, S, Se, ...) spinels it is known that the A and B cations are, to some extent, disordered over the tetrahedral and octahedral lattice sites due to the similar ionic size. It has been shown recently that, for spinel oxides, the ground state structures as well as the disordering effects can be described rather accurately using a simple point-ion electrostatic model[22,23]. In Ref.[23] it is shown that the disorder contribution to the energy of these systems amount to ∼0.03 eV/atom or less at temperatures that are of the order of 1000 K. Therefore, at 298 K these effects can be completely neglected.

C. Influence of spin-orbit coupling

The fact that in our study we include relatively heavy elements such as Sb, Bi, Te, ..., requires a closer look into the effect of the SO coupling on the calculated total energies and on the error cancellation that we systematically improve by introducing the FERE energies of elements. The SO interaction is often considered as purely atomic effect and as already noted all purely atomic contributions to the total energy of the compound or the elemental phases appearing in Eq. (2) should cancel. We show that to a good approximation this statement is true.

Namely, by introducing the SO coupling Eq. (3) can

TABLE IV: Results of our analysis of the influence of spin-orbit coupling on the compound enthalpies of formation. Values (in eV) of the two terms appearing on the right-hand side of Eq. (7), the explicitly calculated SO contribution to the compound total energy ΔE^{SO} and the same contribution expressed as the sum $\sum_i n_i\,\delta\mu_i^{SO}$ of the fitted purely atomic contributions. The analysis has been performed on 61 binary compounds formed out of 21 elements listed in the at the beginning of the table. For pure elements the numbers denote the values of the SO contribution calculated directly for their conventional reference phases and the fitted SO contributions.

Compound	ΔE^{SO}	$\sum_i n_i\,\delta\mu_i^{SO}$	Compound	ΔE^{SO}	$\sum_i n_i\,\delta\mu_i^{SO}$	Compound	ΔE^{SO}	$\sum_i n_i\,\delta\mu_i^{SO}$
Ba	-0.20	-0.21	PtBi	-0.53	-0.60	SnO_2	-0.01	-0.01
La	-0.30	-0.30	PtTe	-0.23	-0.25	SnO	-0.02	-0.02
Hf	-0.70	-0.70	$PtTe_2$	-0.20	-0.20	PbTe	-0.27	-0.30
Ta	-0.73	-0.74	Hg_2Sn	-0.20	-0.19	PbO_2	-0.09	-0.15
Ir	-0.42	-0.42	Hg_2Pb	-0.36	-0.34	PbO	-0.19	-0.24
Pt	-0.42	-0.40	AuSn	-0.18	-0.19	Li_3Sb	-0.01	-0.01
Au	-0.31	-0.32	IrO_2	-0.18	-0.13	Na_3Sb	-0.02	-0.02
Hg	-0.22	-0.26	PtO_2	-0.18	-0.12	Li_2Te	-0.03	-0.03
Sn	-0.06	-0.05	PtO	-0.23	-0.19	Na_2Te	-0.03	-0.03
Pb	-0.56	-0.50	HgO	-0.13	-0.12	Mg_3Bi_2	-0.32	-0.32
Sb	-0.07	-0.06	Mg_2Sn	-0.02	-0.02	MgTe	-0.04	-0.05
Bi	-0.84	-0.79	Mg_2Pb	-0.20	-0.17	AlSn	-0.03	-0.03
Te	-0.11	-0.10	AlSb	-0.03	-0.03	IrN_2	-0.13	-0.13
Li	0.00	0.01	Na_3Bi	-0.20	-0.20	TaN	-0.35	-0.36
Na	0.00	0.00	BeTe	-0.04	-0.05	HfN	-0.34	-0.34
Be	0.00	0.00	$BaBi_3$	-0.71	-0.65	LaN	-0.15	-0.14
Mg	0.00	-0.01	$BaSb_2$	-0.12	-0.11	Ba_2N	-0.14	-0.14
Al	0.00	0.00	$BaSn_2$	-0.11	-0.11	$AuSb_3$	-0.12	-0.13
N	0.00	0.02	BaO	-0.10	-0.10	SnF_4	-0.01	0.01
O	0.00	0.02	BaTe	-0.15	-0.16	PbF_4	-0.07	-0.08
F	0.00	0.02	Ta_3Sb	-0.60	-0.57	BiF_3	-0.10	-0.18
HgTe	-0.20	-0.18	Ta_3Sn	-0.58	-0.57	Li_3Bi	-0.19	-0.19
$IrSn_2$	-0.16	-0.17	$HfTe_2$	-0.30	-0.30	Bi_2O_3	-0.21	-0.31
IrPb	-0.45	-0.46	HfSn	-0.38	-0.38	Sn_3N_4	-0.02	-0.01
IrSb	-0.21	-0.24	LaBi	-0.55	-0.55	AuF_3	-0.11	-0.06
$IrTe_2$	-0.22	-0.20	LaSb	-0.18	-0.18	$AuSb_2$	-0.16	-0.15
PtSn	-0.21	-0.23	SnSb	-0.06	-0.06			
PtPb	-0.42	-0.45	SnTe	-0.07	-0.08			

be written in the following way:

$$\Delta \mathrm{H}_f(\mathrm{A}_{n_1}\mathrm{B}_{n_2}\dots) = \mathrm{E}_{tot.}^{GGA+U}(\mathrm{A}_{n_1}\mathrm{B}_{n_2}\dots) + \Delta E^{SO} - \sum_i n_i\,(\mu_i^{FERE} + \delta\mu_i^{SO}), \quad (6)$$

with ΔE^{SO} and $\delta\mu_i^{SO}$ representing the contributions from the SO coupling to the compound total energy and μ_i^{FERE} values, respectively. The equation (6) can be rewritten in the following way:

$$\Delta \mathrm{H}_f(\mathrm{A}_{n_1}\mathrm{B}_{n_2}\dots) = \Delta \mathrm{H}_f^{FERE}(\mathrm{A}_{n_1}\mathrm{B}_{n_2}\dots) + (\Delta E^{SO} - \sum_i n_i\,\delta\mu_i^{SO}), \quad (7)$$

where the second term on the right-hand side of the equation represents the total SO contribution to the $\Delta \mathrm{H}_f^{FERE}$ that is constructed using the already described procedure without the explicit inclusion of the SO interaction term in the GGA+U Hamiltonian. One could repeat the the whole procedure of solving the least-square problem of Eq. (3) on a set of binary compounds now with the SO interaction included in the Hamiltonian in order to compute the SO contribution defined in Eq. (7). We followed somewhat different, but equivalent approach and fitted directly the $\delta\mu_i^{SO}$ values to reproduce directly computed ΔE^{SO}. Afterwards these fitted elemental contributions are compared with the the real SO contributions calculated directly for the elemental conventional reference phases. This has been done for the set of 21 elements and 61 binary compounds that are shown in Table IV. What we find is that the fitted $\delta\mu_i^{SO}$ agree very well with the directly calculated values. By taking the differences between the two columns of Table IV we find that the av-

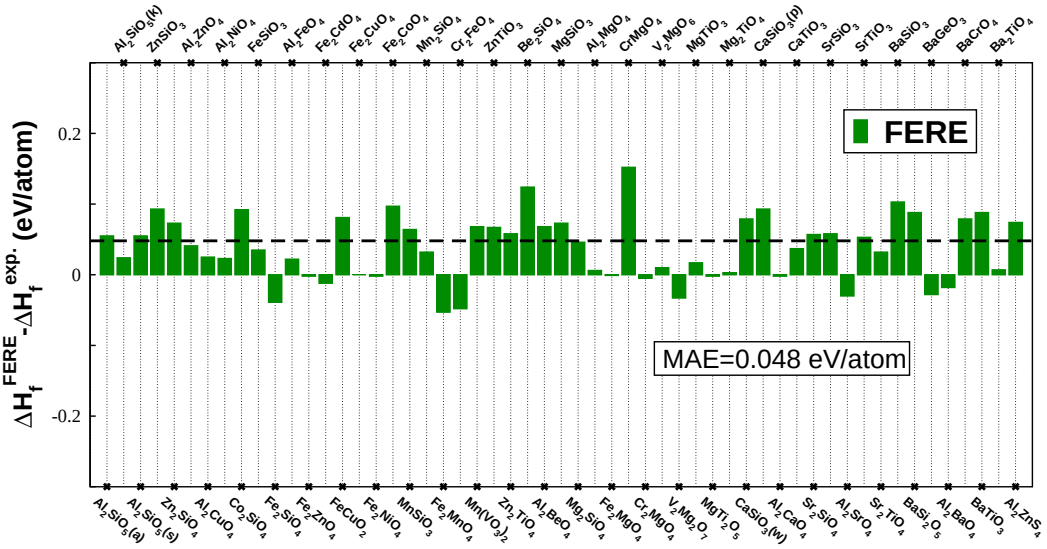

FIG. 4: Histogram showing deviations of ΔH_f^{FERE} (Eq. (5)) relative to $\Delta H_f^{exp.}$ for 55 ternary compounds. Dashed line represent the mean absolute error (MAE) of the method. Numerical values are provided in Table V.

erage absolute value of the parentheses on the right-hand side of Eq. (7) amounts to 0.025 eV/atom. Within the accuracy of the FERE approach (MAE=0.054 eV/atom) the SO contribution can be neglected to a good approximation. This proves that the SO coupling is indeed an atomic quantity which, to a good approximation, does not contribute appreciably to the total energy differences and can be neglected when computing compound ΔH_f.

D. FERE validation

The FERE method has been validated against a set of measured enthalpies of formation for 55 ternary compounds. Results of this *predictivity test* are shown in Fig.4 and in Table V. The calculated MAE=0.048 eV/atom is slightly lower than the value obtained for the fitting set of 252 binary compounds. All but two computed ternary ΔH_f values fall inside the 0.1 eV/atom range (double the MAE). This result implies a good predictive power of the FERE approach when applied to ternary compounds and there is no reason to believe it would not perform as good to any other multinary compound. The two "outliers" are Be_2SiO_4 and $CrMgO_4$ and we suggest that ΔH_f of these two compounds should be revisited experimentally. The interesting fact is that the FERE method captures accurately also the enthalpies of formation of the ternaries that contain two different transition metals (such as Fe_2NiO_4, Fe_2CoO_4, $Mn(VO_3)_2$,...) despite using one single value of the Hubbard U parameter for both. Moreover, the need for the FERE corrections becomes more apparent after comparing FERE performance with that of the GGA+U calculations (same U values that are used throughout this work) MAE of which is 0.29 eV/atom when applied to the same set of ternary compounds (MAE of pure GGA is above 0.4 eV/atom).

VI. APPLICATIONS

A. Thermodynamic stability of solid compounds

As already noted in the introduction, the FERE approach, by providing accurate compound enthalpies of formation, allows for studying compound thermodynamic stability with respect to decomposition into the competing phases. We illustrate this type of application of the FERE method using well characterized, earth abundant mineral Mn_2SiO_4 as an example. To determine the stability of a compound under the thermodynamic equilibrium conditions it is necessary to know the enthalpies of all possible decomposition reactions. If there exists a range of chemical potentials of pure elements within which all these enthalpies have positive values then within this range the studied compound is stable. Mathematically, this means that a following set of inequalities needs to be fulfiled:

$$\begin{aligned} 2\,\Delta\mu_{Mn} + \Delta\mu_{Si} + 4\,\Delta\mu_O &= \Delta H_f(Mn_2SiO_4), \\ \Delta\mu_I &\le 0 \;\; (I = \text{Mn, Si, O}), \\ n_i\,\Delta\mu_{Mn} + m_i\,\Delta\mu_{Si} + q_i\,\Delta\mu_O &\le \Delta H_f(Mn_{n_i}Si_{m_i}O_{q_i}), \\ i &= 1,\ldots,Z, \end{aligned} \tag{8}$$

where $\Delta\mu_I = \mu_i - \mu_i^{FERE}$ is a deviation of the actual elemental chemical potential from its elemental-phase reference, and Z is the total number of competing phases having $\Delta H_f(Mn_{n_i}Si_{m_i}O_{q_i})$ enthalpies of formation. The

TABLE V: Comparison (validation) of ΔH_f values (in eV/atom) from experiment (Refs.[10,11]) and computed using the FERE method for 55 ternary compounds. Conversion factor to kJ/mol is $\sim 96.5*N$, where N stands for the number of atoms per compound formula unit. For $CaSiO_3$ we consider both wollastonite (w) and pseudo-wollastonite (p) structure and for Al_2SiO_5 the three structures appearing in ICSD[20,21] database: Andalusite (a), Kyanite (k) and Silimanite (s), were included in our study.

Compound	ΔH_f^{FERE}	ΔH_f^{exp}	Compound	ΔH_f^{FERE}	ΔH_f^{exp}	Compound	ΔH_f^{FERE}	ΔH_f^{exp}	Compound	ΔH_f^{FERE}	ΔH_f^{exp}
Al_2SiO_5(a)	-3.36	-3.30	$FeCuO_2$	-1.38	-1.30	Mg_2SiO_4	-3.22	-3.17	Sr_2SiO_4	-3.41	-3.35
Al_2SiO_5(k)	-3.31	-3.29	Fe_2CuO_4	-1.43	-1.43	Al_2MgO_4	-3.41	-3.40	$SrSiO_3$	-3.39	-3.33
Al_2SiO_5(s)	-3.36	-3.30	Fe_2NiO_4	-1.60	-1.60	Fe_2MgO_4	-2.11	-2.11	Al_2SrO_4	-3.44	-3.47
$ZnSiO_3$	-2.61	-2.52	Fe_2CoO_4	-1.69	-1.59	$CrMgO_4$	-2.32	-2.17	$SrTiO_3$	-3.47	-3.42
Zn_2SiO_4	-2.42	-2.35	$MnSiO_3$	-2.74	-2.68	Cr_2MgO_4	-2.64	-2.65	Sr_2TiO_4	-3.39	-3.36
Al_2ZnO_4	-3.06	-3.02	Mn_2SiO_4	-2.56	-2.53	V_2MgO_6	-2.54	-2.53	$BaSiO_3$	-3.37	-3.27
Al_2CuO_4	-2.68	-2.66	Fe_2MnO_4	-1.82	-1.87	$V_2Mg_2O_7$	-2.67	-2.70	$BaSi_2O_5$	-3.30	-3.21
Al_2NiO_4	-2.84	-2.82	Cr_2FeO_4	-2.14	-2.19	$MgTiO_3$	-3.26	-3.24	$BaGeO_3$	-2.57	-2.60
Co_2SiO_4	-2.19	-2.10	MnV_2O_6	-2.30	-2.23	$MgTi_2O_5$	-3.25	-3.25	Al_2BaO_4	-3.44	-3.46
$FeSiO_3$	-2.50	-2.47	$ZnTiO_3$	-2.70	-2.63	Mg_2TiO_4	-3.21	-3.21	$BaCrO_4$	-2.50	-2.42
Fe_2SiO_4	-2.19	-2.23	Zn_2TiO_4	-2.44	-2.38	$CaSiO_3$(w)	-3.39	-3.31	$BaTiO_3$	-3.44	-3.35
Al_2FeO_4	-2.95	-2.93	Be_2SiO_4	-3.18	-3.06	$CaSiO_3$(p)	-3.38	-3.29	Ba_2TiO_4	-3.19	-3.18
Fe_2ZnO_4	-1.73	-1.73	Al_2BeO_4	-3.41	-3.34	Al_2CaO_4	-3.44	-3.44	Al_2ZnS_4	-1.43	-1.36
Fe_2CdO_4	-1.58	-1.59	$MgSiO_3$	-3.21	-3.14	$CaTiO_3$	-3.44	-3.40			

first of the inequalities (which is in fact equality) represents the thermodynamic equilibrium condition between the compound and its elemental constituents and sets the allowed ranges of $\Delta\mu_I$ values. This condition, together with the $\Delta\mu_I \leq 0$ requirements, can be represented as the triangle in the three-dimensional $\Delta\mu_I$ space. Projection of this triangle on the $(\Delta\mu_{Mn}, \Delta\mu_{Si})$ plane is shown in Fig. 5(a). The third line of Eq.(8) represents the set of conditions that need to be satisfied in order that it is energetically more favorable the pure elemental substances to form instead of any of the competing phases. These conditions are represented as straight lines in Fig. 5(a), each corresponding to a single competing phase.

We compute $\Delta H_f(Mn_2SiO_4) = -2.56$ eV/atom for the olivine Mn_2SiO_4 which is good agreement with experimental value -2.53 eV/atom (Table V). In addition to the competing binary and ternary compounds listed in Tables II,III and V (MnO, Mn_2O_3, Mn_3O_4, $MnSiO_3$) we compute $\Delta H_f(MnO_2) = -2.47$ eV/atom, $\Delta H_f(Mn_4SiO_7) = -2.18$ eV/atom and $\Delta H_f(Mn_5Si_3O_{12}) = -2.51$ eV/atom. These compounds are reported in the ICSD[20,21], but their enthalpies of formation, to our knowledge, have not been measured. After solving the set of inequalities of Eq. (8) taking into account all reported (in ICSD) competing phases we find ranges of $\Delta\mu_I$ within which Mn_2SiO_4 is thermodynamically stable. Projection of this region on the $(\Delta\mu_{Mn}, \Delta\mu_{Si})$ is shown as the green region in Fig. 5(a) (in the upper right corner). In terms of oxygen chemical potential the green region extends between $-4.07\,\text{eV} < \Delta\mu_O < -3.16\,\text{eV}$. Using the ideal-gas equation of state (pV = nRT) under the assumption of neglecting vibrational degrees of freedom one could derive the dependence of $\Delta\mu_O$ on temperature and oxygen partial pressure as explained in Ref.[24]. Then the green area from Fig. 5(a) can be represented on a p_{O_2} vs. T plot as done in Fig. 5(b). In Ref.[25] the authors report the growing conditions for the artificial Mn_2SiO_4, temperature of $\sim$1600 K and oxygen partial pressure $p_{O_2} = 10^{-10}$ atm. These values are also shown on Fig. 5(b) and are in very good agreement with our predictions.

B. Li-ion battery voltages

We applied our FERE approach also on the problem of predicting accurate Li-ion battery voltages. We tested the predictions against measured average Li intercalation potentials (voltages) for the set of three cathode materials $LiCoO_2$, $LiNiO_2$ and $LiMnPO_4$. The last compound contains PO_4 group in which P appears as a cation and for which we argued that the FERE method should not work. The average Li intercalation potential $\langle V \rangle$ is proportional to the enthalpy of a reaction $Li_{x_1}X \rightarrow Li_{x_2}X + (x_1 - x_2)Li$, when a material Li_xX is delithiated from x_1 to x_2. The equation for the average Li intercalation potential[4] is:

$$\langle V \rangle = \frac{-[E(Li_{x_2}X) - E(Li_{x_1}X) - (x_2 - x_1)\mu(Li)]}{(x_2 - x_1)e}, \quad (9)$$

where E stands for the compound total energies and μ for the total energy of the elemental Li. We find $\langle V \rangle(LiCoO_2)$=4.06 V, $\langle V \rangle(LiNiO_2)$= 3.71 V, and $\langle V \rangle(LiMnPO_4)$= 3.95 V which compares well with experimental results of 4.1[26], 3.9[27], and 4.1 V[28] with the

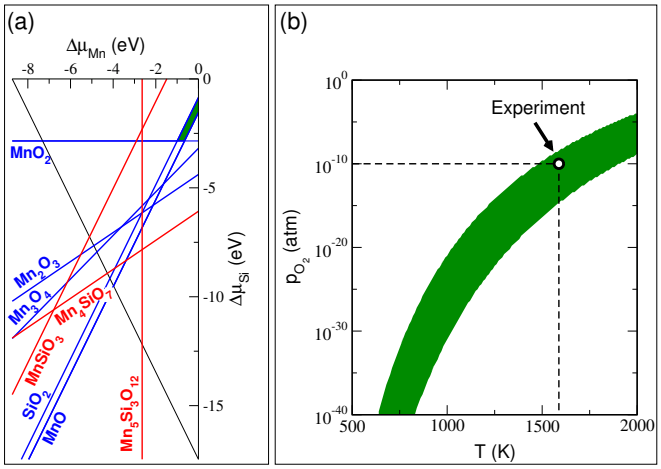

FIG. 5: (a) Projection of the allowed ranges of chemical potentials onto $(\Delta\mu_{Mn}, \Delta\mu_{Si})$ plane with the green polygon defined by Eq. (8) representing the region of thermodynamic stability for Mn_2SiO_4. (b) Stability region from (a) displayed on a oxygen partial pressure versus temperature plot. Experimental growth conditions reported in Ref.[25] are also shown.

average error of 0.13 V similar to the typical experimental error of ∼0.1 V. In these three cases the performance of the FERE approach is similar to the results obtained within pure GGA+U method[4]. Reason for this is that the only pure elemental phase appearing in the equation is elemental Li. We obtained $\delta\mu^{FERE}(\mathrm{Li}) = 0.21$ eV which corresponds to fixed U=3 eV for all transition metals appearing in Eq. (9). The same accuracy can be achieved by using the element dependent U values[31] together with pure GGA value for μ(Li) as shown in Ref.[4]. On the other hand, the following Li intercalation reaction requires a special treatment as noted in Ref.[7]:

$$\mathrm{LiFeF_3} + 2\mathrm{Li} \rightarrow \mathrm{Fe} + 3\mathrm{LiF}, \qquad (10)$$

for which measured electrochemical voltage, half of the enthalpy of the reaction, amounts to 2.5 V. The difficulty here is that there are two pure elemental phases appearing in the reaction Li and Fe. Namely, the pure GGA voltage is calculated to be 2.91 V[29] whereas the GGA+U predicts 3.46 V[7], values that differ considerably from the measured one. In Ref.[7] the value of 2.60 V is calculated by applying the already discussed mixed GGA and GGA+U scheme. After applying our FERE method we compute the electrochemical voltage for the reaction of Eq. (10) of 2.46 V which is in a very good agreement with experiments and as accurate as the mixed GGA/GGA+U scheme.

VII. CONCLUSIONS

In conclusion, we developed a systematic computational scheme based on fitted elemental-phase reference energies for accurate calculation of compound enthalpies of formation. The FERE elemental energies $\{\mu_i^{FERE}\}$ we obtain by solving the least-square problem of Eq. (3) that involves experimental enthalpies of formation. In this way we obtain μ_i^{FERE} for 50 different chemical elements covering the earth most abundant portion of the periodic table. These values are applicable as long as the role of chemical elements as cations or anions is the same as in compounds that belong to the fitting set of 252 binary compounds (groups I-IV cations and V-VII anions) and the GGA+U implementation is equivalent to that used here. The $\{\mu_i^{FERE}\}$ values lead to the MAE=0.054 eV/atom and MAE=0.048 eV/atom when computing enthalpies of formation of the compounds that belong to the fitting set and 55 other ternary compounds, respectively. The main advantage of our approach is in its generality as it applies to different classes of semiconducting and insulating compounds (chalcogenides, halides, pnictides) and in its simplicity. Moreover, it is computationally equivalent to the cost of the simple GGA calculations.

VIII. ACKNOWLEDGMENTS

This research is supported by the U.S. Department of Energy, Office of Basic Energy Sciences, Division of Materials Sciences and Engineering, Energy Frontier Research Centers, under Award DE-AC36-08GO28308 to NREL. This research used high performance computing resources of the National Energy Research Scientific Computing Center, which is supported by the Office of Science of the U.S. Department of Energy under Contract DE-AC02-05CH11231 as well as capabilities of the National Renewable Energy Laboratory Computational Sciences Center, which is supported by the Office of Energy Efficiency and Renewable Energy of the U.S. Department of Energy under Contract DE-AC36-08GO28308.

* Electronic address: stephan.lany@nrel.gov

[1] S. Lany and A. Zunger, Phys. Rev. B **72**, 235104 (2008).
[2] X. Zhang, V. Stevanović, M. d'Avezac, S. Lany, and A. Zunger, unpublished (2011).
[3] X. Zhang, S. Lany, and A. Zunger, unpublished (2011).
[4] V. L. Chevrier, S. P. Ong, R. Armiento, M. K. Y. Chan, and G. Ceder, Phys. Rev. B **82**, 075122 (2010).
[5] J. Yang, A. Sudik, C. Wolverton, and D. J. Siegel, Chem. Soc. Rev. **39**, 656 (2010).
[6] C. Wolverton and V. Ozoliņš, Phys. Rev. B **73**, 144104 (2006).
[7] A. Jain, G. Hautier, S. P. Ong, C. J. Moore, C. C. Fischer, K. A. Persson, and G. Ceder, Phys. Rev. B **84**, 045115 (2011).
[8] P. Seth, L. Ríos, and J. Needs, J. Chem. Phys. **134**, 084105 (2011).
[9] S. Lany, Phys. Rev. B **78**, 245207 (2008).
[10] O. Kubaschewski, C. B. Alcock, and P. I. Spencer, Matherials Thermochemistry, 6th ed. (Pergamon, Oxford, 1983).
[11] D. D. W. et al., J. Phys. Chem. Ref. Data **11**, Supplement No. 2 (1982).
[12] S. Lany, J. Osorio-Guillén, and A. Zunger, Phys. Rev. B **75**, 241203(R) (2007).
[13] L. Wang, T. Maxisch, and C. G, Phys. Rev. B **73**, 195107 (2006).
[14] S. L. Dudarev, G. A. Botton, S. Y. Savrasov, C. J. Humphreys, and A. P. Sutton, Phys. Rev. B **57**, 1505 (1998).
[15] J. Heyd, G. E. Scuseria, and M. Ernzerhof, J. Chem. Phys. **118**, 8207 (2003).
[16] J. P. Perdew, K. Burke, and M. Ernzerhof, Phys. Rev. Lett. **77**, 3865 (1996).
[17] P. E. Blöchl, Phys. Rev. B **50**, 17953 (1994).
[18] G. Kresse and J. Furthmüller, Comput. Mater. Sci. **6**, 15 (1996).
[19] H. J. Monkhorst and J. D. Pack, Phys. Rev. B **13**, 5188 (1976).
[20] G. Bergerhoff and I. Brown, in "Crystallographic Databases", F.H. Allen et al. (Hrsg.) (International Union of Crystallography, Chester, 1987).
[21] A. Belsky, M. Hellenbrandt, V. L. Karen, and P. Luksch, Acta Cryst. **B58**, 364 (2002).
[22] V. Stevanović, M. d'Avezac, and A. Zunger, Phys. Rev. Lett. **105**, 075501 (2010).
[23] V. Stevanović, M. d'Avezac, and A. Zunger, J. Am. Chem. Soc. **133**, 11649 (2011).
[24] J. Osorio-Guillén, S. Lany, S. V. Barabash, and A. Zunger, Phys. Rev. Lett. **96**, 107203 (2006).
[25] C. B. Finch, G. W. Clark, and O. C. Kopp, J. Cryst. Growth **29**, 269 (1975).
[26] G. G. Amatucci, J.-M. Tarescon, and L. C. Klein, J. Electrochem. Soc. **143**, 1114 (1996).
[27] C. D. et al., Int. J. Inorg. Matter. **1**, 11 (1999).
[28] G. H. Li, H. Azuma, and M. Tohda, Electrochem. Solid-State Lett. **5**, A135 (2002).
[29] R. E. Doe, K. A. Persson, Y. S. Meng, and G. Ceder, Chem. Mater. **20**, 5274 (2008).
[30] If we fix U=3 eV for all transition metals (see section V A for justification) the resulting MAE=0.16 eV/atom on the set of 252 binary compounds from Tables II and III. Although, GGA+U improves results, compared to pure GGA, large errors still remain for some transition metal compounds (-0.517 eV/atom for AuCl) as well as for all compounds containing only main group elements for which U=0.
[31] With the value chosen such to reproduce a set of measured heats of chemical reactions that involve the corresponding element

Appendix A: Absolute FERE energies

TABLE VI: The μ_i^{FERE} values (in eV), i.e. the total energies of pure elemental substances in their conventional reference phase. In addition we also show for each element the pseudopotential label (PP) as well as the difference $\delta\mu_i^{FERE} = \mu_i^{FERE} - \mu^{GGA+U}$.

element	PP	μ^{GGA+U}	μ^{FERE}	$\delta\mu^{FERE}$	element	PP	μ^{GGA+U}	μ^{FERE}	$\delta\mu^{FERE}$
Ag	Ag	-0.71	-0.83	-0.12	Mn	Mn	-6.97	-7.00	-0.03
Al	Al	-3.74	-3.02	0.72	N	N	-8.31	-8.51	-0.20
As	As	-4.65	-5.06	-0.41	Na	Na_pv	-1.23	-1.06	0.17
Au	Au	-0.97	-2.23	-1.26	Nb	Nb_pv	-7.04	-6.69	0.36
Ba	Ba_sv	-1.93	-1.39	0.53	Ni	Ni	-3.65	-3.57	0.08
Be	Be	-3.75	-3.40	0.35	O	O_s/O	-4.99/-4.96	-4.76/-4.73	0.23
Bi	Bi_d	-4.06	-4.39	-0.33	P	P	-4.96	-5.64	-0.68
Ca	Ca_pv	-1.93	-1.64	0.29	Pd	Pd	-2.84	-3.12	-0.27
Cd	Cd	-0.91	-0.56	0.35	Pt	Pt	-3.52	-3.95	-0.43
Cl	Cl	-1.79	-1.63	0.16	Rb	Rb_sv	-0.96	-0.68	0.29
Co	Co	-4.65	-4.75	-0.10	Rh	Rh	-4.23	-4.76	-0.53
Cr	Cr_pv	-7.29	-7.22	0.07	S	S	-4.06	-4.00	0.06
Cu	Cu	-2.03	-1.97	0.05	Sb	Sb	-4.12	-4.29	-0.16
F	F	-1.86	-1.70	0.15	Sc	Sc_sv	-5.12	-4.63	0.49
Fe	Fe	- 6.00	-6.15	-0.15	Se	Se	-3.48	-3.55	-0.07
Ga	Ga_d	-3.03	-2.37	0.66	Si	Si	-5.42	-4.99	0.43
Ge	Ge_d	-4.29	-4.14	0.15	Sn	Sn_d	-3.97	-3.79	0.18
Hf	Hf_pv	-8.12	-7.40	0.72	Sr	Sr_sv	-1.68	-1.17	0.51
Hg	Hg	-0.29	-0.12	0.17	Ta	Ta_pv	-9.22	-8.82	0.40
In	In_d	-2.72	-2.31	0.41	Te	Te	-3.14	-3.25	-0.11
Ir	Ir	-5.77	-5.96	-0.19	Ti	Ti_pv	-5.57	-5.52	0.05
K	K_sv	-1.08	-0.80	0.28	V	V_pv	-5.97	-6.42	-0.45
La	La	-3.86	-3.66	0.20	Y	Y_sv	-5.48	-4.81	0.66
Li	Li_sv	-1.86	-1.65	0.21	Zn	Zn	-1.27	-0.84	0.43
Mg	Mg	-1.54	-0.99	0.55	Zr	Zr_sv	-6.60	-5.87	0.72